Opto-Electronics Review

journal homepage: https://journals.pan.pl/opelre

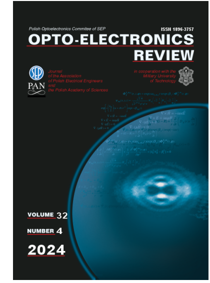

Optimization of MBE-grown GaSb buffer on GaAs substrates for infrared detectors

Dawid Jarosz[1], Ewa Bobko[1*], Małgorzata Trzyna-Sowa[1], Ewa Przeździecka[2], Marcin Stachowicz[2], Marta Ruszała[1], Piotr Krzemiński[1], Anna Juś[1], Kinga Maś[1], Renata Wojnarowska-Nowak[1], Oskar Nowak[1], Daria Gudyka[1], Brajan Tabor[1], Michał Marchewka[1]

[1] Institute of Materials Engineering, Center for Microelectronics and Nanotechnology, University of Rzeszow, al. Rejtana 16, 35-959 Rzeszow, Poland
[2] Institute of Physics, Polish Academy of Sciences, al. Lotników 32/46, 02-668 Warsaw, Poland

Article info:

Article history:
Received 08 Jul. 2024
Received in revised form 24 Jun. 2024
Accepted 24 Sep. 2024
Available on-line 29 Oct. 2024

Keywords:
gallium arsenide;
gallium antimonide;
molecular beam epitaxy;
heteroepitaxy.

Abstract

The aim of this work was to improve the quality of the GaSb buffer layers on GaAs substrates using the molecular beam epitaxy (MBE) technology. The high quality of the GaSb buffer layers is one of the most important elements enabling the synthesis of good quality of type-II superlattices (T2SL) structures for infrared applications. The main challenges in this regard are: compensation of the difference in lattice constants between GaAs and GaSb and obtaining the highest achievable surface quality of the final GaSb layer. In the literature, many authors describe different techniques to obtain the best quality of a GaSb buffer layer. In this work, we present the results of HRXRD, AFM, TOF-SIMS, SEM, and Nomarski optical microscope measurements obtained for 2 µm thick GaSb buffer layers. The GaSb layers are made according to different techniques and these results are compared with a GaSb buffer construction technique according to our own technology. During the processes, we also obtained an unintentional structure of one of the buffer layers, which allowed us to obtain very good results in terms of surface structure and crystallographic quality where FWHM in ω_{RC} scan was equal to 138 arcsec and RMS 0.20 nm proving that there is still a lot of work to be done in this area.

1. Introduction

Type-II strained superlattices (T2SLs) have indeed garnered significant interest as an alternative to existing infrared (IR) detection technologies. T2SLs are a relatively new technology but already show promise in IR applications [1, 2]. The main advantages of the T2SL: can operate across a wide range of wavelengths by manipulating layer thicknesses and composition including the mid-wave and long-wave infrared regions [3, 4]; have the potential for achieving high quantum efficiency, which is crucial for IR detectors [5, 6]; T2SLs do not contain toxic heavy metals such as cadmium or mercury. All of that causes that T2SL have a huge potential as a: infrared detectors such as thermal imaging cameras, motion sensors, security systems, including night heat detection, target recognition; quality control in industry or in medicine such as endoscopy or molecular imaging. However, there are still many problems and challenges which should be solved. One of them is the manufacturing technology. The T2SL structures dedicated for applications include many different group of layers (substrate, buffer layers, electric contact layers, barrier layers, absorber layer, etc.) built with many different materials (in spite of infrared range, final destination, and its complexity of the final architecture) which create together a structure whose parameters determine suitability for applications. One of the problems observed by many authors is the technology for epitaxy of buffer layers to bridge the lattice mismatch between the GaAs substrate and the GaSb layer [7–10]. The most popular substrate used in T2SL structures are GaAs [11] and GaSb [12]. In the case of the GaSb substrates, as were presented by other authors [13,14], the good quality of the GaSb buffers layers should eliminate any defects that may appear on the substrate surface and, as a result, create a perfectly smooth surface.

*corressponding author at: ebobko@ur.edu.pl

https://doi.org/10.24425/opelre.2024.152620
1896-3757/ Association of Polish Electrical Engineers (SEP) and Polish Academic of Sciences (PAS). Published by PAS
© 2024 The Author(s). This is an open access article under the CC BY license http://creativecommons.org/licenses/by/4.0/).

However, in many applications it seems more advantageous to use much cheaper GaAs substrates with a GaSb buffer layer, due to the low IR absorption of the GaAs substrate and the favorable thermal properties of the GaAs [7]. In this case, the main problem is to reduce a large lattice mismatch between the GaAs substrate and the GaSb layer which is equal to 7.8%. Many authors show different methods which allow to obtain a good quality of the GaSb buffer layers on GaAs substrates [7–10]. In the case of Ref. [9], authors propose a procedure for the formation of the GaSb layer using an interfacial misfit (IMF) matrix enriched with Be dopant. In the mentioned case, 60-degree dislocations are trapped on Be atoms which blocks their propagation to the surface of the GaSb buffer layer. Other approach was proposed by Hao *et al*. [10] which used the I-type of AlSb/GaSb superlattice in the initial phase of the growth to reduce the lattice mismatch. Some other ideas were explored by Jasik *et al*. [7,8], which aim was to obtain good quality of a buffer layer, and to this end, the authors proposed and evidenced a necessity of lowering substrate temperature to optimal for GaSb just before interruption of the GaAs layer growth. Lee *et al*. [15] propose to grow the GaSb buffer using a three-step ZnTe buffer layer. The main purpose of all these methods, beside reducing the lattice mismatch is also production of the relative thin buffer layers (which allows to reduce the cost and the time) but with the best possibly parameters and the best possible surface quality. The quality of the surface influences the quality of the next layers that create a whole T2SL. From the point of view of application, the surface quality is dedicated to defects in T2SL and thus determined, for example, the amount of dark current. Fluctuations in carrier concentration and associated dark currents produce noise. Additionally, dark current increases power consumption, cooling requirements and read-out challenges.

In this paper, we present the results collected for different GaSb 2 µm thick buffer layers obtained by different methods described in literature. We made it in the same MBE machine and compared these results with the experimental results obtained for GaSb buffer layers synthesised by our method. Our investigation for one of the samples also shows that non-intentional manner allow to get much better results than other described below, however, in our opinion, such situation is rather random and difficult to repeat. Nevertheless, it provides additional information that may allow to achieve even better buffer layers in the future than those currently produced.

2. Experimental and methods

For the purpose of this work, a set of six different GaSb buffer layers were deposited by MBE [Riber Compact 21T (III-V)] and characterised. Five of the samples in the set labelled M1, M2, M3, M4, M5 are heteroepitaxial GaSb layers with a thickness of about 2 µm deposited on a GaAs substrate, while the last sample labelled H1 is a homoepitaxial GaSb layer deposited on a GaSb substrate. Heteroepitaxial GaSb layers were deposited on 1/4 of 2" GaAs:Un (100) substrates 1SP (one-side polished) with a thickness of 350 µm at 510°C. For heteroepitaxial structures, a GaAs refresh layer of 200 nm thickness was deposited under optimal growth parameters such as a substrate temperature of 590°C, the flux ratio V/III = 16.78 and a growth rate of approximately 1000 nm/h described in detail in our previous work [16]. Homoepitaxial GaSb layers were deposited on ¼ of 2" GaSb:Te 1SP (100) substrate with a thickness of 500 µm. Homoepitaxial GaSb layer was deposited at a substrate temperature measured by a pyrometer of 530°C measured during wetting of the substrate with a flux of Sb. The establishment of the growth temperature was realized with an IR pyrometer IRCON, which spectral response peak is at 930 nm, and measuring range is in between 450°C and 1200°C. Pyrometer calibrations were performed for both GaAs and GaSb substrates by observing the RHEED pattern upon desorption of oxides from the substrate surface at 580°C and 566°C, respectively. All samples have been made using a solid source Riber Compact 21T (III-V) MBE system, equipped with standard ABN60 dual-zone effusion cells for In, Al, Ga and with a valved arsenic and antimonic cracker: VAC 500 and VCOR 300, respectively. The Be-doped cell is a standard ABN35 effusion cell with one heater. The substrates rotation speed during growth was set to 10 rpm (rotations per minute). The substrates temperature ramp rate was 10°C/min during the heat-up and 20°C/min during the cool-down processes. All samples were characterised by atomic force microscope INNOVA BRUKER, scanning electron microscope (SEM) HELIOS NANOLAB650, optical microscope with differential interference contrast (DIC) OLYMPUS DSX1000, high-resolution X-ray diffractometer EMPYREAN 3. Time-of-flight secondary ion mass spectrometer (TOF-SIMS) 5, IONTOF measurements were also taken for the samples labelled M3, M3*, and M5.

M1: Buffer GaSb is an MBE growth of a GaSb metamorphic layer [8]. In this case, in the first step, after deoxidation of the GaAs substrate, a 200 nm GaAs buffer layer is applied under optimized growth conditions for homoepitaxial GaAs layers, such as Ga flux, As flux, and a substrate temperature of 590°C [16]. At the end of the GaAs buffer layer, the substrate temperature is lowered to 510°C and then the growth of the GaAs buffer is interrupted by cutting off the gallium flux. In the next step, the arsenic flux is replaced by an optimal antymony flux for the growth of homoepitaxial GaSb layers. In the final step, the growth of the GaSb layer is initiated by providing a gallium flux with an optimal value for the growth of homoepitaxial GaSb layers [8].

M2: Buffer GaSb is a GaSb layer growth using an IMF matrix [9,17]. In M2 buffer, in the first step, after deoxidizing the GaAs substrate, a 200 nm GaAs buffer layer is applied under optimized growth conditions for homoepitaxial GaAs layers, the same like in M1 buffer layer condition [16]. The growth of the GaAs buffer is then interrupted by cutting off the gallium and arsenic fluxes reduced for 20 s. The GaAs buffer layer is then wetted with an antimony flux of the optimum value for the growth of homoepitaxial GaSb layers. In the next step, the substrate temperature is lowered to 510°C. In the final step, the growth of a GaSb layer is initiated by providing a gallium flux of the optimal value for the growth of homoepitaxial GaSb layers [9,17].

M3: Buffer GaSb according to the Polish patent application P.443805 [18]. In the first step, after deoxidation of the GaAs substrate, a 200 nm GaAs buffer layer is grown under optimized growth conditions for homoepitaxial GaAs

layers, such as Ga flux, As flux, and a substrate temperature of 590°C for a growth rate of about 1 µm/h limited by the gallium flux. Then, without interrupting the growth of the GaAs layer, the growth rate of the GaAs layer is reduced to a value of about 120 nm/h by decreasing the gallium flux and the arsenic flux while maintaining the mutual ratio V/III of about 16.78. The next step is to reduce the substrate temperature from 590°C without interrupting the growth of the GaAs layer within 3 min to the optimal value for the growth of GaSb layers equal to 510°C and to interrupt the growth process after by cutting off the gallium flux. Then, after wetting the surface with arsenic flux for 1 s, the arsenic flux is changed to the antimony flux suitable for the growth of GaSb layers and wetting the surface with it for 1 min. In the next step, the growth of a 400 nm GaSb layer doped with beryllium with a linear fading concentration of 1e19 cm^{-3} to 1e18 cm^{-3} is started under optimized growth conditions such as substrate temperature 510°C and antimony/gallium flux ratio 7.29 for a growth rate of about 400 nm/h limited by the gallium flux. This was followed by a 40 nm layer of GaSb doped with beryllium with an exponential decay in concentration from 1e18 cm^{-3} to 1e17 cm^{-3}. Finally, a 1600 nm layer of pure GaSb grown under optimized growth conditions such as substrate temperature 530°C and antimony/gallium flux ratio for a growth rate of about 400 nm/h limited by the gallium flux. It should be noted that when converting group V from As flux to Sb flux, the pyrometer readings change from 510°C to 530°C despite the constant temperature maintained on the main furnace.

M3*: Buffer GaSb is a repeat of the M3 process.

M4: Buffer GaSb is a growth of a GaSb layer on the transition layer from AlSb (5 nm) / GaSb (5 nm) superlattices. In the first step, after deoxidation of the GaAs substrate, a 200 nm GaAs buffer layer is applied under the same paprameters like in case of buffer M1, M2. The growth of the GaAs buffer is then interrupted by cutting off the gallium flux. In the next step, the substrate temperature is lowered to 510°C. In the next step, the arsenic flux is replaced by an antimony flux of the optimum value for the growth of AlSb layers. Growth of a 5 nm AlSb layer is started at the values of aluminum and antimony fluxes optimal for the AlSb layer and then a 5 nm GaSb layer is started at the gallium and antimony fluxes optimal for it. The sequence of AlSb/GaSb layers is repeated 40 times. In the final stage, the growth of the GaSb layer begins [10].

M5: Buffer GaSb is a growth of a beryllium-doped GaSb layer giving carrier concentrations of 5e18 cm^{-3}. In the first step, after deoxidizing the GaAs substrate, a 200 nm GaAs buffer layer is applied under optimized growth conditions for homoepitaxial GaAs layers, such as Ga flux, As flux, and a substrate temperature of 590°C. The growth of the GaAs buffer is then interrupted by cutting off the gallium and arsenic fluxes for 20 s. The GaAs buffer layer is then wetted with an antimony flux of the optimum value for the growth of homoepitaxial GaSb layers. In the next step, the substrate temperature is lowered to 510°C. In the final step, the growth of a beryllium-doped GaSb layer with doping level at 5e18 cm^{-3} is initiated by providing a gallium flux of the optimal value for the growth of homoepitaxial GaSb layers and a beryllium flux to achieve a carrier concentration of p = 5e18 cm^{-3} [9].

H1: Buffer GaSb is a homoepitaxial GaSb layer made under optimal growth conditions such as a reciprocal V/III flux ratio of about 6.29 and a substrate temperature of 530°C for a growth rate of about 400 nm/h limited by the gallium flux.

Figure 1 shows schematics of the compared GaSb epitaxial layers deposited on GaAs substrates according to five selected methods and one homoepitaxial layer.

3. Results and discussion

Regardless of the chosen method, the first step to obtaining a heteroepitaxial GaSb buffer layer on a GaAs substrate was to develop optimal growth conditions for homoepitaxial layers: GaAs and GaSb. Figure 2 shows a table of the growth parameters that were used during the work associated with this article. Increasing the temperature gradient on a Ga effusion cell from 100°C to 150°C for GaAs layers and from 100°C to 200°C for GaSb layers improves the surface morphology, respectively. Therefore, we considered this parameter important. On the left is a summary of the surface morphology from the three characterisation methods: Nomarski, SEM, AFM for homoepitaxial GaAs (sample K176) (a) and GaSb (sample K186) (b) layers.

Seven GaSb buffer layers with thicknesses of approximately 2 µm according to procedures labelled as: M1, M2, M3, M3*, M4, M5, and H1 was grown in the same MBE machine. Due to the anomaly, it is necessary to state the chronological order of fabrication of the individual layers

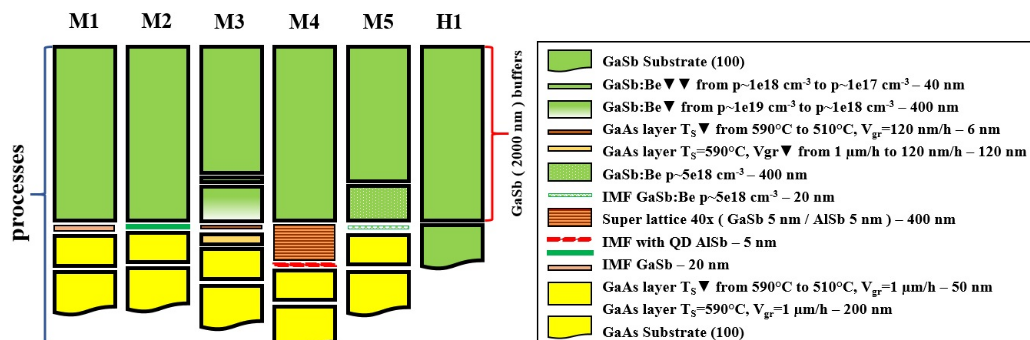

Fig. 1. Schematics of the compared GaSb epitaxial layers deposited on GaAs substrates according to five selected methods and one homoepitaxial layer.

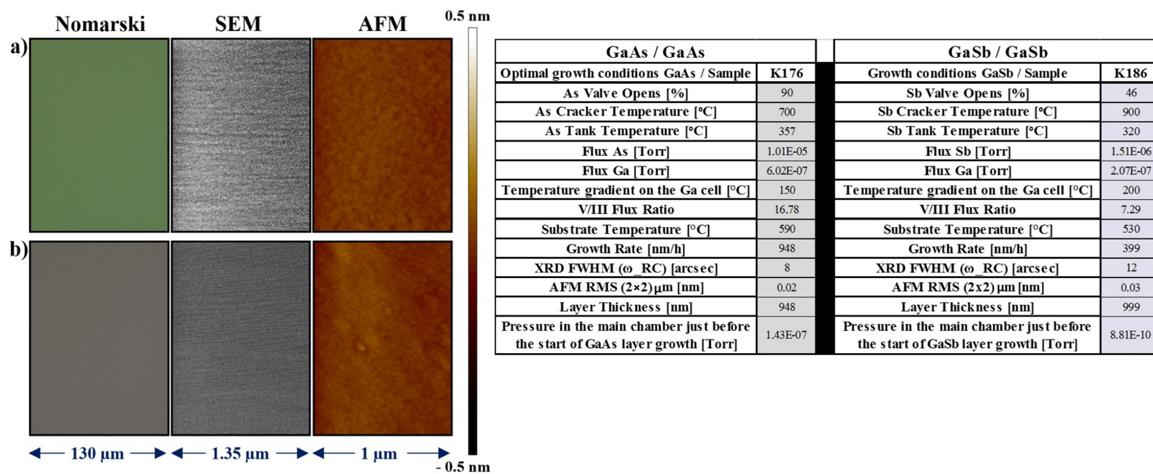

GaAs / GaAs	
Optimal growth conditions GaAs / Sample	K176
As Valve Opens [%]	90
As Cracker Temperature [°C]	700
As Tank Temperature [°C]	357
Flux As [Torr]	1.01E-05
Flux Ga [Torr]	6.02E-07
Temperature gradient on the Ga cell [°C]	150
V/III Flux Ratio	16.78
Substrate Temperature [°C]	590
Growth Rate [nm/h]	948
XRD FWHM (ω_RC) [arcsec]	8
AFM RMS (2×2)µm [nm]	0.02
Layer Thickness [nm]	948
Pressure in the main chamber just before the start of GaAs layer growth [Torr]	1.43E-07

GaSb / GaSb	
Growth conditions GaSb / Sample	K186
Sb Valve Opens [%]	46
Sb Cracker Temperature [°C]	900
Sb Tank Temperature [°C]	320
Flux Sb [Torr]	1.51E-06
Flux Ga [Torr]	2.07E-07
Temperature gradient on the Ga cell [°C]	200
V/III Flux Ratio	7.29
Substrate Temperature [°C]	530
Growth Rate [nm/h]	399
XRD FWHM (ω_RC) [arcsec]	12
AFM RMS (2x2) µm [nm]	0.03
Layer Thickness [nm]	999
Pressure in the main chamber just before the start of GaSb layer growth [Torr]	8.81E-10

Fig. 2. Summary of surface morphology: Nomarski optical microscope, SEM, AFM for homoepitaxial layers. Image scales are provided under each method, while colour scales for AFM measurements are provided on the right. The table shows the growth parameters for GaAs of about 1 µm homoepitaxial layers deposited on 1/4 of 2" GaAs:Un (100) 1SP substrate with a thickness of 350 µm (left side) and the growth parameters for GaSb homoepitaxial layers deposited on 1/4 GaSb:Te (100) 1SP substrate with a thickness of 500 µm. (a) GaAs around 1 µm labelled as K176, (b) GaSb around 1 µm labelled as K186.

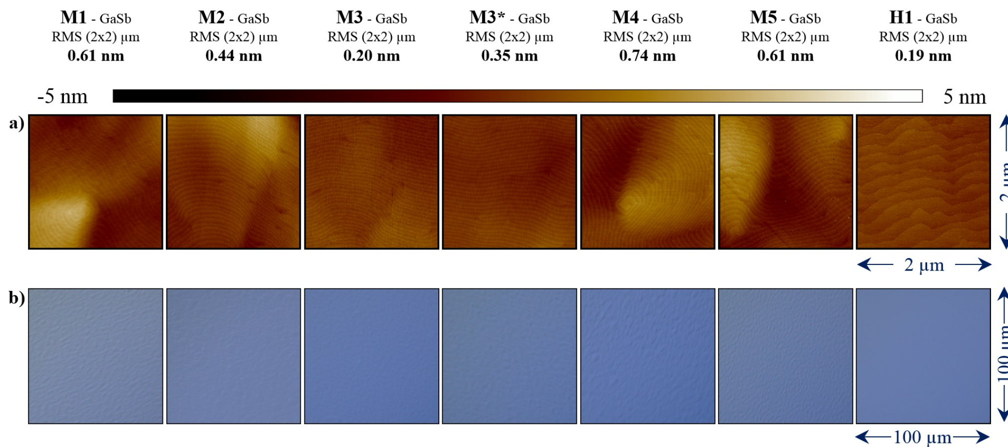

Fig. 3. Surface morphology from GaSb buffer layers with a thickness of about 2 µm made according to the described methods labelled as: M1, M2, M3, M3* M4, M5, and H1 obtained from AFM measurements (a) and Nomarski optical microscope measurements (b). The surface roughness from the AFM for a (2×2) µm scan is shown under the method designation. Sample M3* was a repeat of the M3 process.

which was as follows: H1, M1, M2, M4, M5, M3, two other processes including from Be and M3*. Figure 3 summarises the AFM measurements (a) and optical measurements (b) for each of the 2 µm GaSb layers. The surface roughness values obtained from the AFM for the scan from the (2×2) µm area are included under the labels of each procedure. Compared to H1, the best performing method was the one labelled M3 achieving a surface roughness of 0.20 nm, while the repeat process labelled M3* had a roughness of 0.35 nm. For these layers, no helical dislocations were observed on the surface on the AFM scans taken from the (10×10) µm region while they were frequently observed for methods: M1, M4, M5, and occasionally on M2.

The next step was to compare the crystallographic properties of the deposited layers shown in Fig. 4, after taking an ω_{RC} scan and determining the value of the half-width of the FWHM peak coming from the GaSb layer. For the homoepitaxial layer designated H1, the FWHM was only 12 arcsec which was measured for comparison with heteroepitaxial layers. The smallest FWHM of the layer is achieved for the process labelled M3. It was 138 arcsec - the best value compared to other methods. The M3 process was repeated and described as M3*, which achieved a more similar FWHM value to the others of 176 arcsec, which was still the best result. The FWHM values were as follows: 190, 214, 197, and 200 arcsec for M1, M2, M4, and M5 samples, respectively.

The value obtained by us for M3* equal to FWHM = 176 arcsec for a 2 µm GaSb layer is almost identical to the work of Benyahia *et al*. [19]. In the literature, [20] reported FWHM of 194 arcsec and 20 arcsec of GaSb layers which thickness is of 0.5 µm and 5 µm, respectively. On the other hand, Li *et al*. [21] reported FWHM of 160 arcsec for a GaSb layer with a 1 µm thickness and a growth rate of 1 µm/h. Jasik *et al*. [7, 8] reported FWHM of 160 arcsec for a GaSb layer with a 2.5 µm thickness and FWHM of 196 arcsec for a GaSb layer with a 1.5 µm thickness.

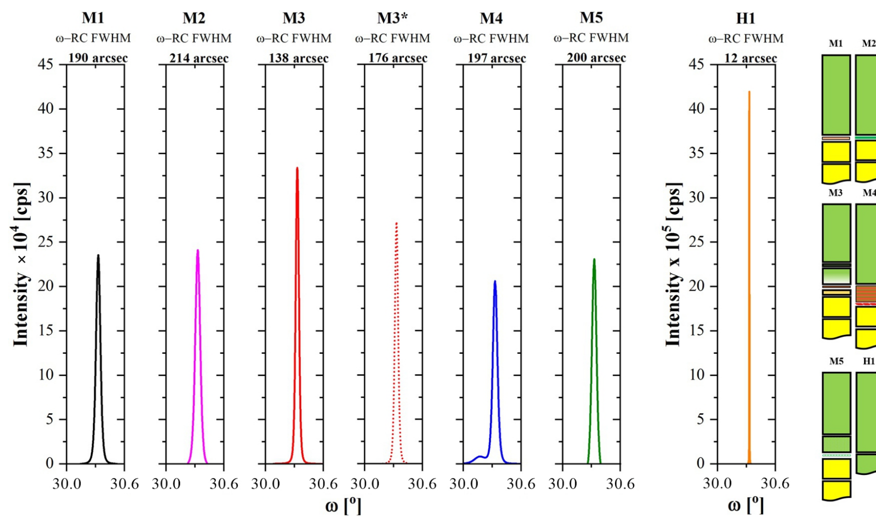

Fig. 4. HR-XRD measurements in ω_{RC} scans for GaSb buffer layers with a thickness of about 2 µm made according to methods labelled as: M1, M2, M3, M3*, M4, M5, and H1. The half-widths of the peaks originating from the GaSb layers are shown under the method designation. A schematic representation of each layer is shown on the right. The M3* process was a repeat of the M3 process.

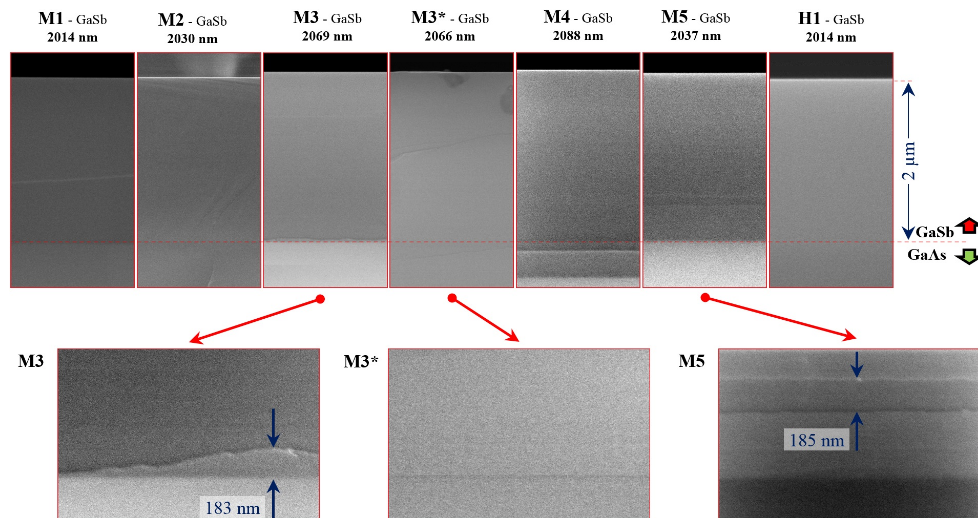

Fig. 5. SEM images from a cross-section of GaSb layers deposited according to the method described as: M1, M2, M3, M3*, M4, M5, and H1. The red dotted line indicates the location of the GaSb/GaAs layer interface. For the method labelled M4, this is the interface between the GaSb/AlSb superlattice layer and the GaSb layer. The thickness of the GaSb layer is indicated under the method designation. In the second line, magnified areas from the SEM image showing the unintended effect of an additional layer in the process labelled M3, its absence in the repeated process labelled M3* and the unwanted layer in the process preceding M3 labelled M5 are included.

Further SEM measurements visible in Fig. 5 from a cross-section of the deposited GaSb layers confirmed their thicknesses at about 2 µm of: 2014, 2030, 2069, 2066, 2088, 2037, 2014 nm for M1, M2, M3, M3*, M4, M5, H1, respectively. In addition, they revealed the possible reason for the unusual FWHM value for the GaSb layer labelled M3. During the M3 process, the formation of an unintentional layer with a developed surface and a thickness ranging from a few to as much as 185 nm took place. We suspect that this unintentional layer was the reason for the significant improvement in the crystalline quality of the GaSb layer compared to the other processes. The appearance of the unintentional layer must have been related to the first use of the Be effusion cell after along period of downtime. For the M5 process, which chronologically preceded the M3 process, a similar unintentional layer with a thickness of about 185 nm but an undeveloped surface was visible at a distance of about 400 nm from the GaSb / GaAs interface, which coincides exactly with the closure of the Be shutter heated to about 850°C. We suspect that the use of a doped Be effusion cell without prior degassing the shutter after a long waiting period, resulted in the uncontrolled evaporation of the material deposited on the shutter and its unintentional incorporation during the growth of the GaSb layer in the process designated M5.

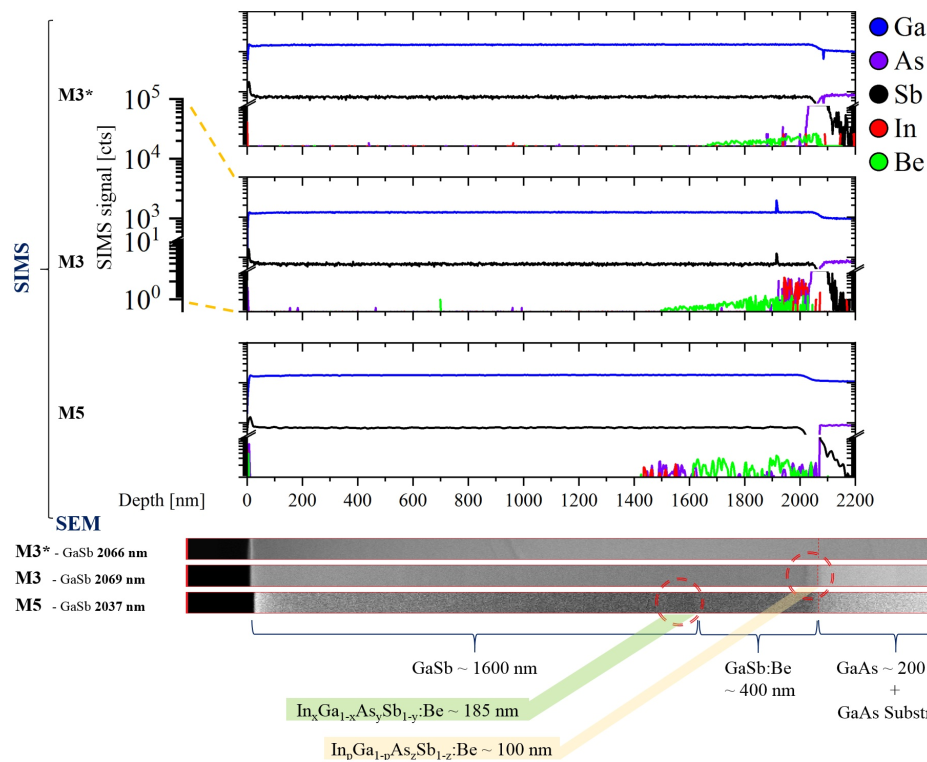

Fig. 6. TOF-SIMS depth profile analysis of three GaSb buffer layers designated M3*, M3, and M5. The layers were performed in chronological order: M5 then M3 then two other processes including from Be and a repeat of M3 labelled as M3*. For a better localisation of the origin of the SIMS analysis signals, sections from the SEM images are included below at an appropriate scale. The unintentionally generated areas are marked with a red circle on the SEM image.

In the process designated M3, the Be effusion cell was heated to about 900°C and it was cooled during the growth of the first 400 nm of the GaSb layer. During the closure of the Be shutter, the temperature of the beryllium efusion cell was 720°C, and therefore no anomalies were observed above 400 nm from the GaSb / GaAs interface. Heating the Be cell to 900°C just prior to the start of a GaSb layer growth in the process designated M3 resulted in the formation of an unintentional layer of material evaporated from the Be shutter on the GaAs surface. The unintentional layer with a developed surface and not fully defined composition allowed the deposition of a GaSb buffer layer with the best crystallographic parameters and surface morphology. For the M5, M3, and M3* processes, depth analysis using TOF-SIMS was performed to estimate the nature of the unintentional layers appearing in the M5 and M3 processes and undetected M3*. Figure 6 includes the SEM in depth profiles at an appropriately sized scale to better showing areas of signal origin for TOF-SIMS analysis. The analysis presented additional unintentional presence of In and As in the areas marked with a red circle in the SEM image for M3 and M5 processes with the signal strength from In and As being at least twice as high for process M3 compared to M5. For the repeated M3 process, labelled M3*, additional signal from In and As not occurred.

4. Conclusions

Seven GaSb buffer layers with a thickness of approximately 2 µm including six heteroepitaxial layers on a GaAs substrate were deposited and in the same MBE machine and thus directly compared. Based on the comparative analysis, the optimal method for depositing a 2 µm GaSb buffer layer directly on a GaAs substrate, designated M3, was selected. The results clearly show that our method, assuming the same thickness, is better from the point of view of the crysthallographic parameters and surfaces morphology. The necessity of degassing the shutters, in this case Be, before working with the doped cell was demonstrated in order to avoid the possibility of the formation of unintentional but desirable layer of not fully defined composition. Based on TOF-SIMS depth analysis, it was estimated that the unintentional layers in the M3 and M5 processes are most likely quaternary Be-doped layers: $In_xGa_{1-x}As_ySb_{1-y}$:Be in the M5 process and $In_pGa_{1-p}As_zSb_{1-z}$:Be in the M3 process with $(p > x)$ and $(z > y)$. Based on the presented study, we believe that the pre-applied quaternary InGaAsSb:Be layer directly on GaAs can significantly improve the quality of the GaSb layer. In such case, 138 arcsec FWHM in ω_{RC} and 0.20 rms value was obtained. In order to reduce the lattice mismatch between the substrate and the target layer, so-called gradient buffers can be used: linear or step buffers [22–24]. The use of multi-component layers, e.g., InGaAsSb, offers the possibility to manipulate the crystal lattice parameters by changing the composition of the individual elements.

Author's statement

Conceptualization of this study, original writing and original draft, analysis of results, writing, review and editing, supervision, investigation of the MBE growth and methodol-

ogy, D.J.; review and editing, analysis of the results, M.M.; analysis of the results, E.P. and MS.; HR-XRD measurements and analysis of the results, E.B. and M.R.; SEM measurements, P.K.; AFM measurements, A.J.; optical measurements, contact profilometer measurements, K.M and R.W.N.; TOF-SIMS measurements, M.T.S.; student assisting during MBE growth processes and characterisation processes of test samples, O.N., D.G. and B.T.

Acknowledgements

This research was funded under projects no. POIR.04.01.04-00-0123/17 and no. SKN/SP/601031/2024.

References

[1] Razeghi, M. *et al.* State-of-the-art type II antimonide-based superlattice photodiodes for infrared detection and imaging. *Proc. SPIE* **7467**, 7467OT (2009). https://doi.org/10.1117/12.828421.

[2] Plis, E. A. InAs/GaSb Type-II Superlattice Detectors. *Adv. Electron.* (2014). https://doi.org/10.1155/2014/246769.

[3] Rogalski, A., Kopytko, M. & Martyniuk, P. InAs/GaSb type-II superlattice infrared detectors: three decades of development. *Proc. SPIE* **10177**, 1017715 (2017). https://doi.org/10.1117/12.2272817.

[4] Wei, Y., Gin, A., Razeghi, M. & Brown, G. Advanced InAs/GaSb superlattice photovoltaic detectors for very long wavelength infrared applications. *Appl. Phys. Lett.* **80**, 3262–3264 (2002). https://doi.org/10.1063/1.1476395.

[5] Hostut, M. & Ergun, Y. Quantum efficiency contributions for type-II InAs/GaSb SL photodetectors. *Phys. E: Low-Dimens. Syst. Nanostructures* **130**, 114721 (2021). https://doi.org/10.1016/j.physe.2021.114721.

[6] Xiaochao, L. *et al.* Atomic intermixing and segregation at the interface of InAs/GaSb type II superlattices. *Superlattices Microstruct.* **104** (2017). https://doi.org/0.1016/j.spmi.2017.02.052.

[7] Jasik, A. *et al.* Comprehensive investigation of the interfacial misfit array formation in GaSb/GaAs material system. *Appl. Phys. A* **124**, 512 (2018). https://doi.org/10.1007/s00339-018-1931-8.

[8] Jasik, A. *et al.* Atomically smooth interfaces of type-II InAs/GaSb superlattice on metamorphic GaSb buffer grown in 2D mode on GaAs substrate using MBE. *Curr. Appl. Phys.* **19**, 120–127 (2019). https://doi.org/10.1016/j.cap.2018.11.017.

[9] Gutierrez, M., Araujo, D., Jurczak, P., Wu, J. & Liu, H. Solid solution strengthening in GaSb/GaAs: A mode to reduce the TD density through Be-doping. *Appl. Phys. Lett.* **110**, 092103 (2017). https://doi.org/10.1063/1.4977489.

[10] Hao, R. *et al.* Molecular beam epitaxy of GaSb on GaAs substrates with AlSb/GaSb compound buffer layers. *Thin Solid Films* **519**, 228–230 (2010). https://doi.org/10.1016/j.tsf.2010.08.001.

[11] Plis, E. *et al.* Mid-infrared InAs/GaSb strained layer superlattice detectors with nBn design grown on a GaAs substrate. *Semicond. Sci. Technol.* **25**, 085010 (2010). https://doi.org/10.1088/0268-1242/25/8/085010.

[12] Delmas, M., Debnath, M., Liang, B. & Huffaker, D. Material and device characterization of Type-II InAs/GaSb superlattice infrared detectors. *Infrared Phys. Technol.* **94**, 286–290 (2018). https://doi.org/10.1016/j.infrared.2018.09.012.

[13] Koerperick, E., Murray, L., Norton, D., Boggess, T. & Prineas, J. Optimization of MBE-grown GaSb buffer layers and surface effects of antimony stabilization flux. *J. Cryst. Growth* **312**, 185–191 (2010). https://doi.org/10.1016/j.jcrysgro.2009.10.033.

[14] Jasik, A. *et al.* MBE Growth of Type-II InAs/GaSb Superlattices on GaSb Buffer. In *Crystal Growth: Theory, Mechanisms and Morphology*, 293–327 (Nova Science Publishers, Incorporated, 2012).

[15] Lee, W. *et al.* Molecular beam epitaxy of GaSb layers on GaAs (001) substrates by using three-step ZnTe buffer layers. *J. Cryst. Growth* **305**, 40–44 (2007). https://doi.org/10.1016/j.jcrysgro.2007.04.015.

[16] Jarosz, D. *et al.* Initial optimization of the growth conditions of GaAs homo-epitaxial layers after cleaning and restarting the molecular beam epitaxy reactor. *ACS Omega* **8**, 32998–33005 (2023). https://doi.org/10.1021/acsomega.3c04777.

[17] Huang, S. H. *et al.* Strain relief by periodic misfit arrays for low defect density GaSb on GaAs. *Appl. Phys. Lett.* **88**, 131911 (2006). https://doi.org/10.1063/1.2172742.

[18] Jarosz, D. *et al.* Method of producing GaSb layers on GaAs substrates (2023). P.443805, Polish Patent Application.

[19] Benyahia, D. *et al.* Low-temperature growth of GaSb epilayers on GaAs (001) by molecular beam epitaxy. *Opto-Electron. Rev.* **24**, 40–45 (2016). https://doi.org/10.1515/oere-2016-0007.

[20] Jallipalli, A. *et al.* Structural analysis of highly relaxed GaSb grown on GaAs substrates with periodic interfacial array of 90° misfit dislocations. *Nanoscale Res Lett.* **4** (2009). https://doi.org/10.1007/s11671-009-9420-9.

[21] Li, Y. *et al.* Molecular beam epitaxial growth and characterization of GaSb layers on GaAs (0 0 1) substrates. *Appl. Surf. Sci.* **258**, 6571–6575 (2012). https://doi.org/10.1016/j.apsusc.2012.03.081.

[22] Araujo, D., Gonzalez, D., Garcia, R., Sacedon, A. & Calleja, E. Dislocation behavior in InGaAs step- and alternating step-graded structures: Design rules for buffer fabrication. *Appl. Phys. Lett.* **67**, 3632–3634 (1995). https://doi.org/10.1063/1.115341.

[23] Gonzalez, D., Aragon, G., Araujo, D. & Garcia, R. Control of phase modulation in InGaAs epilayers. *Appl. Phys. Lett.* **76**, 3236–3238 (2000). https://doi.org/10.1063/1.126592.

[24] Shang, X. Z. *et al.* Low temperature step-graded InAlAs/GaAs metamorphic buffer layers grown by molecular beam epitaxy. *J. Phys. D: Appl. Phys.* **39**, 1800 (2006). https://doi.org/10.1088/0022-3727/39/9/015.